Original Research

Novel insights into the role of 5-Methylcytosine RNA methylation in human abdominal aortic aneurysm

Yuchen He[1], Hao Zhang[2], Fanxing Yin[2], Panpan Guo[2], Shiyue Wang[1], Yihao Wu[2], Shijie Xin[1], Yanshuo Han[2,*,†], Jian Zhang[1,*,†]

[1]*Department of Vascular Surgery, The First Hospital of China Medical University, 110001 Shenyang, Liaoning, China,*
[2]*School of Life and Pharmaceutical Sciences, Dalian University of Technology, 116001 Dalian, Liaoning, China*

TABLE OF CONTENTS

1. Abstract

Background: It remains largely unclear about the function of 5-methylcytosine (m5C) RNA modification in the context of abdominal aortic aneurysm (AAA). In this regard, the present work focused on investigating m5C RNA methylation and related modulator expression levels in AAA. **Materials and methods**: To this end, we quantified the m5C methylation levels in AAA tissues (n = 32) and normal aortic tissues (n = 12) to examine the mRNA m5C status and m5C modulator expression at mRNA and protein levels. Meanwhile, mod-

ulator localization within AAA tissue samples was detected by immunohistochemistry (IHC). Moreover, RNA immunoprecipitation-sequencing (RIP-seq) was also used to analyze the lncRNAs and mRNA binding to Aly/REF, as an m5C reader. **Results**: m5C expression markedly elevated in AAA in comparison with normal aortic samples in the AAA cases. The major 5-methylcytosine modulators, including *NSUN2, NSUN5,* and *Aly/REF,* which represented the major parameters related to the abnormal m5C modification level, were observed up-regulating in AAA tissues at both protein and mRNA levels. In addition, *NSUN2* mRNA level remarkably related to *Aly/REF* expression, and they were co-expressed in the same cells in AAA group. Regarding the cellular location, Aly/REF was associated with inflammatory (CD45+, CD3+) infiltrates. Simultaneously, after screening for reads in AAA tissue compare with anti-Aly/REF group relative to IgG as control, we obtained totally 477 differentially expressed Aly/REF-binding lncRNAs and 369 differentially expressed Aly/REF-binding mRNAs in AAA tissue. The functions of Aly/REF-interacting lncRNA were involved in immune system process and macrophages infiltration. Through regulatory network (lncRNA-mRNA) analysis, our findings predicted the potential mechanism of Aly/REF-induced lncBCL2L1 and Aly/REF-lncFHL1 axis in AAA and inspire the understanding of m5C and lncRNA in AAA. **Conclusions**: This study is the first to examine m5A modification within human AAA samples. Our results indicate that m5C modulators, namely, Aly/REF and NUSN2, play vital parts in the human AAA pathogenic mechanism, which shed new lights on the function of m5C modification within AAA. Taken together, findings in this work offer a possible RNA methylation modification mechanism within clinical AAA.

2. Introduction

Abdominal aortic aneurysm (AAA) accounts for a primary cause leading to cardiovascular event among the old male population [1, 2]. AAA is featured by the local while persistent abdominal aortic weakening and expansion [3], and it may be symptomatic, asymptomatic, or may present as rupture. The open retroperitoneal or transperitoneal selection operation has been the frequently adopted repair method [4]. Nonetheless, it is now suggested that the placement of the endoluminal stent graft in aneurysm may be applied in replacement of open intervention [5, 6]. There is no effective pharmacological treatment capable of limiting AAA progression or avoiding AAAs rupture. So far, pharmacological intervention is unavailable, while monitoring aneurysm size prior to operation is the only choice [7].

The pathogenic mechanism of AAA has been suggested to be complicated and multifactorial. In previous studies, AAA is suggested to be related to the deficient ad-

ventitial/medial arterial layers, like fibroblasts and smooth muscle cells (SMCs). Recent research with either human tissue or animal models has led to a shift regarding AAA, and AAA development is now considered to be part of a significant and dynamic remodeling process in the vessel [8]. Moreover, the critical pathological features are vascular inflammation [9], oxidative stress (OS) [10], aortic extracellular matrix (ECM) destruction [11], and aortic wall thinning due to vascular smooth muscle cell (VSMC) losses [12].

Epigenetic alterations, such as DNA methylation [13], histone modification [14] or RNA modification [15], has been found to exert vital parts in AAA due to their strong impacts on regulating gene levels. N6-methyladenosine (m6A) has been well investigated and most frequently observed in mRNA, which is found to be related to pre-mRNA translation, processing, mRNA decay and miRNA biogenesis. m6A modifications are reversible and dynamic among mammalian cells, and they are suggested to be the other epigenetic regulating layer associated with histone and DNA modifications [16, 17]. Our recent study has reported that aberrant RNA epigenetic modifications, such as m6A RNA methylation, are present in AAA [18]. The above results can shed novel lights on the AAA pathogenic mechanism.

Compared with m6A modification, 5-methylcytosine (m5C) is rarely investigated. m5C may be discovered in mRNA, tRNAs, rRNAs and recently poly(A)RNAs. It represents the abnormal RNA modification existing in various RNA species, such as numerous non-coding RNAs (ncRNAs), mitochondrial and cytoplasmic ribosomal RNAs (rRNAs), enhancer RNAs (eRNAs), transfer RNAs (tRNAs) and messenger RNAs (mRNAs) [19, 20]. m5C is a vital factor to regulate gene expression, like ribosomal assembly, RNA export, RNA stability and translation [21–23].

Hence in this study, we focused on the function of m5C mRNA modification involved in human AAA tissues, and detected m5C mRNA methylation level as well as related modulator expression. In addition, this study examined the relationship of m5C modification with the clinical data of patients. Moreover, RNA immunoprecipitation-sequencing (RIP-seq) was also used to analyze the lncRNAs and mRNA binding to Aly/REF, and to investigate the role of m5C RNA methylation in progression of AAA.

3. Materials and methods

3.1 China Medical University Aneurysm Biobank and tissue collection

This study obtained human AAA tissue and relevant peripheral blood samples from altogether 147 consecutive cases at the Department of Vascular Surgery, The First Hospital of China Medical University (CMU) following the open operation for aneurysm according to previous descrip-

Table 1. Primer sequences used for reverse-transcription polymerase chain reaction.

Gene	Forward primer	Reverse primer
NSUN1	AAGGGTGCCGAGACAGAACT	GAGCACGACTAGACAGCCTC
NSUN2	CAAGCTGTTCGAGCACTACTAC	CTCCCTGAGAGCGTCCATGA
NSUN5	CGCTACCATGAGGTCCACTAC	GCATCTCGCACCACGTCTT
NSUN6	TCTCAGCCCTTCATTTGACAGT	TCCAGTGCTATAACTTCTCCCTG
Dnmt1	TGCCAAGACGATTGAAGGCAT	GCAGGGAGGGCTCATTAAAAT
Aly/REF	TATGATCGCTCTGGTCGCAG	AGAGGGACGCCGTTGTACT
GAPDH	ACAACTTTGGTATCGTGGAAGG	GCCATCACGCCACAGTTTC

tion from January 2009 to December 2020 [18, 24]. In addition, each case provided the informed consent for participation. All human AAA samples were collected in line with guidelines from the World Medical Association Declaration of Helsinki. The Ethics Committees of the First Hospital of CMU approved our study protocol (ethical approval number: 2019-97-2).

We collected aneurysm tissues from 147 Chinese AAA cases at the time of emergency or elective open surgical repair. In addition, we obtained the clinical and history data from all patients, like medication history, rupture history, peripheral/coronary artery disease history, or risk factors like hypertension, smoking, hyperlipidemia and diabetes mellitus (DM). Meanwhile, patients with concurrent Marfan syndrome, Ehlers-Danlos syndrome, or additional identified connective tissue or vascular diseases were excluded from this study. Within 147 AAAs, for present study, 32 AAA tissues (28 male patients and 4 female patients) were available for further analyses. For inclusive 32 AAA patients, AAA was analyzed by computed tomography angiography (CTA). For all AAA cases, their diameter of infra-renal abdominal aorta was over 30 mm or 1.5–2 folds as high as the abdominal aorta diameter in corresponding normal segment [25] under CTA diagnosis. Furthermore, the included patients had no evidence or medical history of any cancer disease.

Over the same period, abdominal aorta samples from 12 heart-beating brain-dead organ donors (10 males and 2 females) were used as the controls. For controls, those with concurrent drug history, cancer, infection and additional immune-related disorders potentially affecting this work were excluded.

3.2 RNA extraction and total mRNA m5C level determination

TRIzol reagent (TaKaRa Bio, Shiga, Japan) was utilized to extract total mRNA from aortic tissues according to the standard protocol as described previously. The extracted total mRNA was used to directly detect the m5c RNA methylation level by adopting the fluorometricm m5C RNA methylation ELISA kit (Epigentek, Farmingdale, NY, USA). Briefly, a pipette was utilized to add mRNA (200 ng) in the detection wells. Later, an m5C detection complex solution with a specific m5c antibody was added to the wells. After washing, the wells were added with flu-

orescence development solution for incubation under ambient temperature away from direct light. The fluorescence development solution will turn pink in the presence of sufficient m5c products. The fluorescence was read on a fluorescence microplate reader within 2 to 10 min at 530EX/590EM nm. Then, the mRNA m5C methylation level was assessed through the m5c-modified mRNA proportion in overall mRNA (m5C%) following the specific instructions.

3.3 Quantitative real-time PCR analysis

For the high-quality RNAs, their A260/A280 ratio was greater than 1.8. The PrimeScript RT Master Mix (Q711-02/03, Vazyme Biotech, Nanjing, China) was used to synthesize cDNA from total mRNA, and the Universal SYBR qPCR Master Mix (Q711-02/03, Vazyme Biotech, Nanjing, China) was utilized to conduct quantitative real-time PCR (qRT-PCR) in LightCycler 480 system (Roche Molecular Systems, Indianapolis, IN, USA) in accordance with the amplification protocols after modification. The PCR conditions were as follows, 30 s of initial denaturation under 95 °C; followed by 5 s of denaturation under 95 °C, and 30 s of annealing and 30 s of extension under 60 °C for 40 cycles. RT-PCR was conducted for twice or more for all samples. GAPDH served as the internal control. Each primer was provided by Sangon (Shanghai, China): *NSUN1, NSUN2; NSUN5, NSUN6, Dnmt1* and *Aly/REF*, and their sequences are shown in Table 1. An improvement of the 2ˆ (–delta delta CT) method for quantitative real-time polymerase chain reaction data analysis.

3.4 Western blotting analysis

The RIPA-based reagents were utilized to extract proteins from fresh frozen tissues in line with specific instructions; later, the concentration of each sample was measured by a Pierce BCA Protein Assay kit. The samples were isolated through SDS-PAGE, followed by transfer onto PVDF membranes. Afterwards, membranes were blocked using skimmed milk and incubated using suitable primary as well as secondary antibodies. Later, the ECL detection system was employed for membrane developing in line with specific instructions. GAPDH was used for normalization. In the present work, the following primary antibodies were utilized, anti-Aly/REF (ab202894; Abcam, Cambridge, UK; dilution 1:1000) and anti-NSUN2

Table 2. Demographic and clinical characteristics of AAA patients and controls group included in this study.

Characteristics	AAA group (N = 32)		Control group (N = 12)		p
Baseline	n	mean ± SD (%)	n	mean ± SD (%)	
Age, Year	32/32	61.94 ± 8.38	12/12	58.67 ± 10.72	0.279
female	4/32	12.50%	2/12	16.67%	0.529
BMI	31/32	25.75 ± 4.37	11/12	24.41 ± 5.58	0.344
maximum AAA diameter, mm	32/32	74.23 ± 4.44	NA	NA	NA
Comorbidity					
Hypertension	17/32	53.13%	5/12	41.67%	0.368
Smoking	18/31	58.06%	5/12	41.67%	0.265
Hyperlipidemia	5/32	15.63%	1/12	8.33%	0.471
Diabetes mellitus	1/32	3.13%	0/12	0%	0.727
Cardiac disease	4/31	12.90%	1/12	8.33%	0.569
Renal disease	2/31	6.45%	0/12	0%	0.515
Medication use	10/32	31.25%	1/12	0%	0.118

Note, AAA, abdominal aortic aneurysm; SD, standard deviation; BMI, body mass index; NA, not available.

(Cat. No. 20854-1-AP; Proteintech, Wuhan, China; dilution 1:1000) and anti-GAPDH (dilution 1:2000; Zsbio, Beijing, China). The densitometry was performed with Image J software (Java 1.8.0_172, National Institutes of Health, Bethesda, Rockville, MD, USA) and normalized to the signal intensity of GAPDH for equal protein loading control of each sample in each experiment.

3.5 Histological and Immunohistochemical (IHC) analyses

The typical 2–3-μm aortic tissue sections were utilized to carry out histological and IHC analyses. In brief, we used hematoxylin-eosin (HE) to stain paraffin-embedded sections for assessing the inflammatory cell composition, morphology and infiltration extent in each AAA sample according to previous description [14].

In IHC assay, antigen retrieval was performed through boiling tissue sections in sodium citrate solution (pH = 6.0), after washing, suitable antibodies were used to treat the sections, then they were deparaffinized and hydrated. To analyze cells within AAA wall, endothelial cells (ECs) were analyzed by anti-CD34 (1:100; Proteintech, Wuhan, China), SMCs were measured through anti-α-SMA (1:400; Absin, Shanghai, China), T-lymphocytes were detected through anti-CD3 (1:800; Absin Bioscience, Shanghai, China), while leukocytes were examined by anti-CD45 (1:500; Proteintech, Wuhan, China). In addition, m5c modulator expression within AAA tissues was detected by adopting anti-Aly/REF and anti-NSUN2 in line with specific protocols.

The Nikon ScanScope 90i system (Nikon, Melville, NY, USA) was used to obtain the digital images of the stained tissues (slides). To be specific, the settings for digital image capturing were 20×/40× magnification and 5-slide load capacity for the 90i system.

To conduct standard and traditional staining, the extent of calcification and cellularity of vascular wall were characterized for histological classification. Thereafter, ba-sic cell count and related cell intensity were used to evaluate the grade, such as new vessel formation, infiltrates and SMCs.

To determine the expression of biomarkers in single cells in aneurysms, we made successive slides of every sample and incubated them using appropriate antibodies. In all cases, one slide was stained with an antibody to detect a certain cell type; thereafter, the anti-biomarker antibodies were used to stain the successive slides.

3.6 Immunofluorescence (IF) staining of NSUN2 and Aly/REF

In brief, typical 2–3-μm paraffin-embedded sections were subjected to deparaffinate and rehydration with gradient ethanol, followed by boiling within citrate buffer (pH = 6.0) for retrieving the antigen epitopes, rinsing by PBS, and overnight incubation using the rabbit anti-Aly/REF antibody (1:400; Abcam, Shanghai, China) under 4 °C within the humid chamber. After rinsing by Tris-buffered saline thrice, the Alexa Fluor® 488 (green) affiniPure fab fragment goat anti-rabbit antibody (dilution 1:400; Jackson ImmunoResearch Laboratories, West Grove, NJ, USA) was used to incubate the sections for an hour. Then sections were washed 3 times with Tris-buffered saline, and incubated with rabbit anti-NSUN2 antibody (dilution 1:100; Proteintech, Wuhan, China) overnight at 4 °C in a humidified chamber. Sections were washed 3 times with Tris-buffered saline and incubated with CY3 (red) conjugated goat anti-rabbit antibody (dilution 1:300; Servicebio, Wuhan, China) was used to further incubate the membranes for 1 h. The sections were washed 3 times again, and stained by DAPI. At last, the confocal microscope (Nikon CI plus, Tokyo, Japan) was used to obtain sections.

3.7 RNA Immunoprecipitation sequencing (RIP-seq)

First of all, the Magna RIP™ RNA-binding Protein Immunoprecipitation Kit (Millipore, Billerica, MA, USA) was utilized for RIP-seq in line with specific in-

structions. In brief, after coating with 10 μg anti-Aly/Ref antibody (ab202894, Abcam, Cambridge, UK) or corresponding IgG antibody (Millipore, Billerica, MA, USA), cell lysates were used to incubate the coated magnetic beads overnight under 4 °C. Later, the proteinase K digestion buffer was used to treat the RNA-protein complexes. Thereafter, the phenol: chloroform: isoamyl alcohol was used to purify the coprecipitated RNAs, and the RNA content and purity were analyzed by adopting NanoDrop 2000c [26]. Additionally, we eliminated rRNAs out of the immunoprecipitated RNAs; later, the rRNA-depleted RNAs were used to input RNA samples through the NEBNext® Ultra™ II Directional RNA Library Prep Kit (New England Biolabs, Inc., Ipswich, MA, USA) in accordance with specific protocols. In addition, the BioAnalyzer 2100 system (Agilent Technologies, Inc., Palo Alto, CA, USA) was utilized to analyze the quantity and quality of libraries. At last, we loaded the clustered libraries on the reagent cartridge to carry out sequencing using the illumina Hiseq 4000 (Illumina, San Diego, CA, USA) system by the use of 150 bp paired-end reads. Then, Q30 was utilized for quality control. Finally, the Cloud-Seq Biotech (Shanghai, China) was applied in RIP-RNA-Seq high-throughput sequencing.

With regard to mRNA and lncRNA, we used hisat2 software to align high-quality reads to human reference genome (UCSC hg19). Thereafter, we adopted Cuffdiff (version 2.1.0: http://cole-trapnell-lab.github.io/cufflinks/) for obtaining the fragments per kilobase of transcript per million mapped reads (FPKM) under the guidance of Ensembl gtf gene expression profiles, which were the mRNA and lncRNA expression profiles [27]. Further, we determined p-values and fold changes (FCs) according to FPKM, and discovered the differentially expressed mRNAs and lncRNAs. The target genes of lncRNAs were estimated according to their locations relative to adjacent genes. Additionally, the predicted target genes were subjected to GO (www.geneontology.org) and KEGG (www.genome.jp/kegg) enrichment to determine the major functions and related pathways involved in differentially expressed mRNAs and lncRNAs on the basis of differentially expressed mRNAs.

3.8 LncRNA and mRNA interaction network analysis

Since the expression of lncRNAs shows significant relation with the surrounding protein encoding genes, numerous lncRNAs play roles of the cis regulators [28]. LncRNA and its adjacent mRNAs were integrated and differentially expressed in the biome to explore the function of lncRNA. LncExpDB (https://ngdc.cncb.ac.cn/lncexpdb) estimates lncRNA genes' expression reliability and capacities, used for the lncRNA-mRNA interaction network analysis.

3.9 PPI network construction and visualization

PPI networks can offer precious data about cell functions or the signal transduction pathways. In this study, we searched the interactions of DEGs-encoded proteins through the Search Tool for the Retrieval of Interacting Genes/Proteins (http://string-db.org/) online database. Thereafter, the PPI network was built using 5 calculation algorithms (EPC, Degree, EcCentricity, MNC and MCC) and visualized using Cytoscape (http://cytoscape.org/). At last, those overlapping genes obtained by the above 5 algorithms encoded core proteins that had vital biological regulatory activities.

3.10 Statistical analysis

Statistical analysis was completed using SPSS22.0 (SPSS Inc., Chicago, IL, USA). Differences among the categorical variables were compared by chi-square test between groups. In addition, the one-sample Kolmogorov-Smirnov test was used to examine the distribution of data. Later, the non-parametric Mann–Whitney U test or parametric t-test for unpaired samples was used for analysis according to variable distribution. Thereafter, partial correlation analysis was conducted to examine the associations among continuous variables after adjusting for smoking, age and sex. Correlations between continuous variables were quantified by using Spearman's rank correlation coefficient. A difference of $p < 0.05$ suggested statistical significance.

4. Results

4.1 Characterization of AAA subjects and histological analysis

Table 2 presents the clinical and demographic data of AAA cases and normal subjects. For AAA cases, their age ranged from 43 to 86 years, and the average AAA maximum diameter was found to be 69.25 ± 20.37 mm. None of the control subject (age ranged 41 to 73) showed any signs of atherosclerosis and no evidence or medical history of aneurysm and the other vascular disorders was known. Age, sex, and body mass index (BMI) were comparable between two groups. At the same time, differences in concurrent diseases, i.e., Hypertension, hyperlipidemia, and renal diseases, were not significant.

The symptoms of the AAA patients are summarized in Table 2. Altogether 22% AAA cases had aneurysmal rupture, whereas 5 out of the 32 cases had iliac aneurysms. Among AAA cases, each AAA sample was semi-quantitatively and histologically characterized for evaluating each histopathological characteristic degree within AAA wall as previously [14]. In Table 3, IHC was used to differentiate between the four main cell types in AAAs, i.e., endothelial cells, lymphocytes, macrophages, and smooth muscle cells to assess the extension of the individual histopathological features in AAA wall.
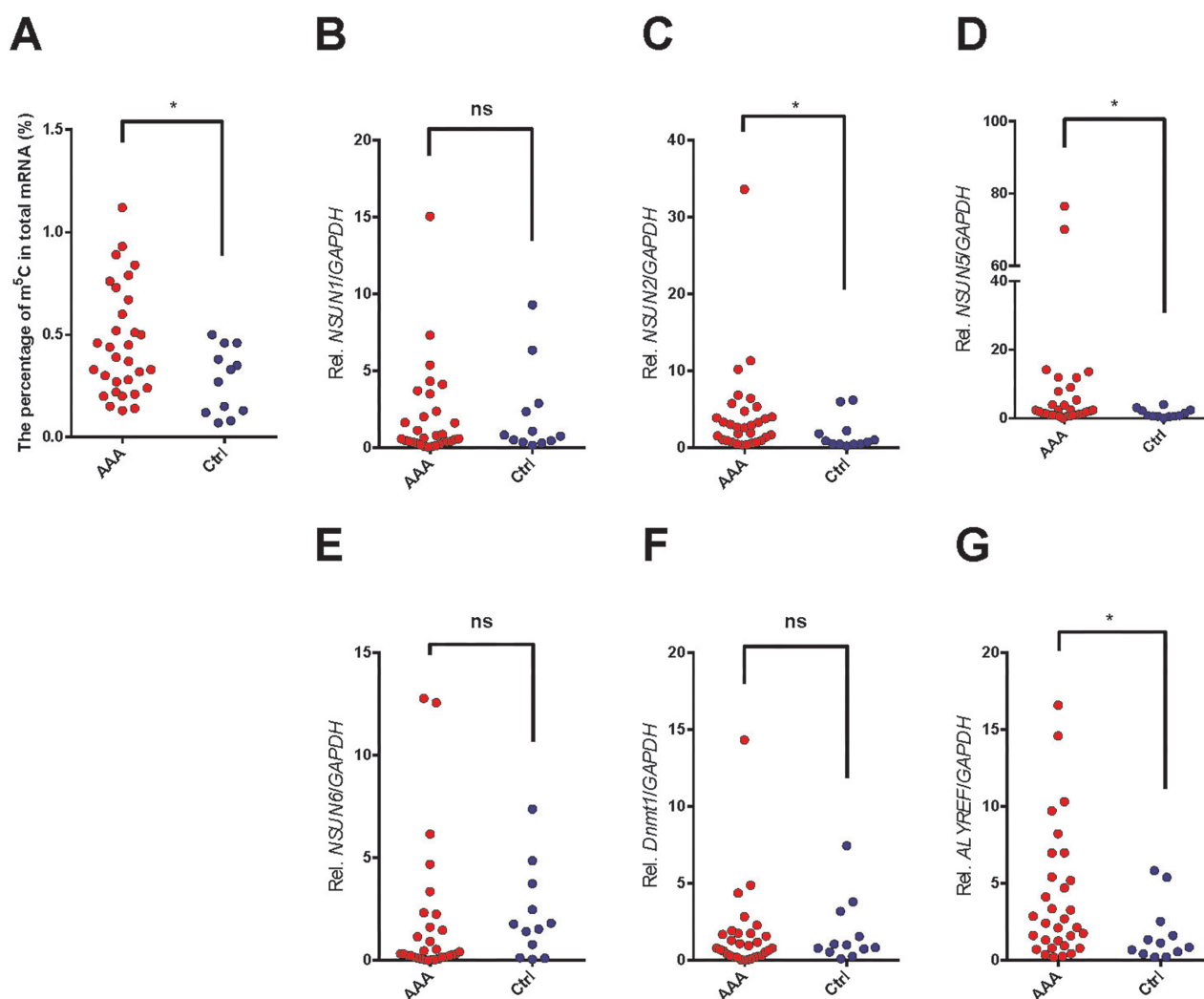
Fig. 1. Expression of m5C RNA methylation status (A) and m5C methylation modulators (B, C, D, E, F, and G) at the mRNA level in AAA tissue samples compared with the healthy control aortas analyzed by qRT-PCR. The non-parametric Mann-Whitney U test was all applied to analyze the m5C methylation ratio (A); the m5C "writers" family, *NSUN1* (B), *NSUN2* (C), *NSUN5* (D), *NSUN6* (E), *Dnmt2* (F); and "readers" family *Aly/REF* (G). The expression of individual m5C RNA methylation modulators related to the expression of GAPDH set as 1 (100% expression). *, $p < 0.05$; **, $p < 0.01$. m5C, 5-Methylcytosine RNA methylation; AAA, abdominal aortic aneurysm; qRT-PCR, quantitative real-time polymerase chain reaction; ns, not significant.

4.2 Increased m5c mRNA methylation occurred in AAA tissue samples

According to our analysis, relative m5c mRNA methylation level within AAA tissues showed significant correlation with an increased m5c proportion in the overall mRNA relative to controls (more than 1.5-fold; $p = 0.040$; Fig. 1A).

4.3 The mRNA expression of m5c modulators in AAA tissue samples and association with clinical data

Thereafter, certain typical molecules that might be related to m5C mRNA modification were analyzed for their expression at mRNA level, including *NSUN1, NSUN2, NSUN5, NSUN6, Dnmt2* and *Aly/REF* (Fig. 1B–G). In the current study, the mRNA expressions of *NSUN2, NSUN5*

and *Aly/REF* were observed up-regulating in the AAA tissue samples relative to matched normal tissues (>2 folds, $p = 0.037$; 2 folds, $p = 0.035$; 2 folds, $p = 0.046$). Differences in *NSUN1, NSUN6* and *Dnmt1* mRNA levels were not significant ($p = 0.645$, $p = 0.136$ and $p = 0.448$).

4.4 The correlations among the mRNA m5C status and mRNA expression levels of m5Cc modulators in AAA tissue samples

According to our results, the m5C% in total mRNA was significantly correlated with NSUN2, NSUN5 and *Aly/REF* expression levels (R = 0.316, 0.320, and 0.312 respectively, and $p = 0.039$, $p = 0.037$ and $p = 0.042$, respectively; Table 4). Afterwards, the associations of mRNA expression were examined. As a result, *NSUN2* mRNA ex-

Table 3. Histological characterization of all AAA tissue samples.

No.	Abdominal pain	Pulsating sensations in the abdomen	Comorbidity-Iliac artery aneurysms	Ruptured AAA	Cellularity (HE)	Infiltrates (CD45)	Macrophages (CD68)	SMCs (α-SMA)	Neovessel (CD34)
A1	√				+	+/++	+ (+/++)	++	+ (+/++)
A2		√			+/–	+	+ (+/–)	+/++	+/++
A3	√				+	+	–/+	++/+++	+/–
A4	√				+/++	++++	+ (+/–)	+/++	+++
A5					++	+/–	++	+/–	–/+
A6	√					+/++	+/++	+/–	+++
A7	√				+/++	++++	++	++ (+/++)	+/++
A8		√			+/–	+/++	–/+	+	+
A9		√			+	++	–	+/–	+ (+/–)
A10	√				+/–	+/–	+	+/–	–/+
A11	√				+/++	+++	+	+	++/+++
A12	√	√		√	+	+/++	–/+	+/–	+/++
A13		√			++	+	+ (+/–)	+/++	–/+
A14	√		√		+	++++	+/–	+/–	+/–
A15		√			+/++	++++	+ (+/–)	+	+/++
A16			√		+	+/++	+/–	+/++	+/–
A17	√			√	+	++ (+/++)	+ (+/–)	+/++	+/++
A18	√	√			+/–	+++	+	+ (+/–)	+
A19	√			√	++	+/++	–	+	+++
A20					+	+	+/–	++	++
A21	√			√	+	+/–	+	+ (+/–)	–/+
A22	√				++	+++	–/+	+	++
A24		√			+/++	++	+	+/++	+
A25	√	√	√	√	+/–	+++	–/+	+/++	+/–
A26	√			√	+	+	+/++	+	+/++
A27		√	√		+	+++	+/++	+	–/+
A29	√				+/–	+	++	+/++	+ (+/–)
A30					+	+/–	+/++	+/++	+
A31					+/–	+++	++	+/–	+ (+/–)
A32	√		√		+	++ (+/++)	+	+/–	–/+
A33	√	√		√	+/++	+	–/+	+	+++

pression showed significant relationship with the expressions of *NSUN5* and *Aly/REF* (R = 0.538, $p < 0.001$ and R = 0.464, $p = 0.002$ respectively). *Aly/REF* expression significantly correlated with *NSUN1*, *NSUN5*, and *NSUN6* (R = 0.313, 0.642 and 0.339; $p = 0.041$, $p < 0.001$ and $p = 0.026$, respectively) Table 4.

Thereafter, the associations of m5C modulator expression levels with clinical features were analyzed. Similarly, the expression of *NSUN1, NSUN2, NUSN5, NSUN6* and *Dnmt1* positively correlated to platelet hematocrit (PCT) (R = 0.429, 0.429, 0.462, 0.494, and 0.537; $p = 0.016, 0.016, 0.009, 0.005$, and 0.002, respectively).

NSUN5, NSUN6, and *Dnmt1* expression significantly correlated to platelets count (PLT) (R = 0.443, 0.456, and 0.382; $p = 0.013, 0.010$, and 0.034, respectively). The expression of *NSUN1* and *NSUN5* at mRNA level were negative associated with mean corpuscular volume (MCV), the correlation coefficient was –0.470 and –0.419 ($p = 0.008$ and 0.019 respectively) in Fig. 2.

4.5 The protein expressions of mRNA m5C modulators and their cellular colocalization in AAA tissues

We selectively performed western blot analysis for NSUN2 and Aly/REF, because their roles on the 5-mC modification in mRNA, their expressions at mRNA levels and their interrelatedness with mRNA m5C status in human AAA tissue samples. Fig. 3A displays the representative images of NSUN2 and Aly/REF expression levels measured through Western blotting (**Supplementary Fig. 1**). Aly/REF and NSUN2 protein expression markedly increased within AAA tissues relative to normal controls (more than 1.5-fold for both comparison; $p = 0.039$, and $p = 0.003$, respectively; Fig. 3B,C).

Similarly, significantly increased expressions of NSUN2 and Aly/REF were also observed in AAA tissue samples, both were observed in the healthy aorta tissue through IHC analysis, date was not shown. Additionally, we examined the colocalization of NSUN2 and Aly/REF within the successive sections by IHC. As a result, NSUN2
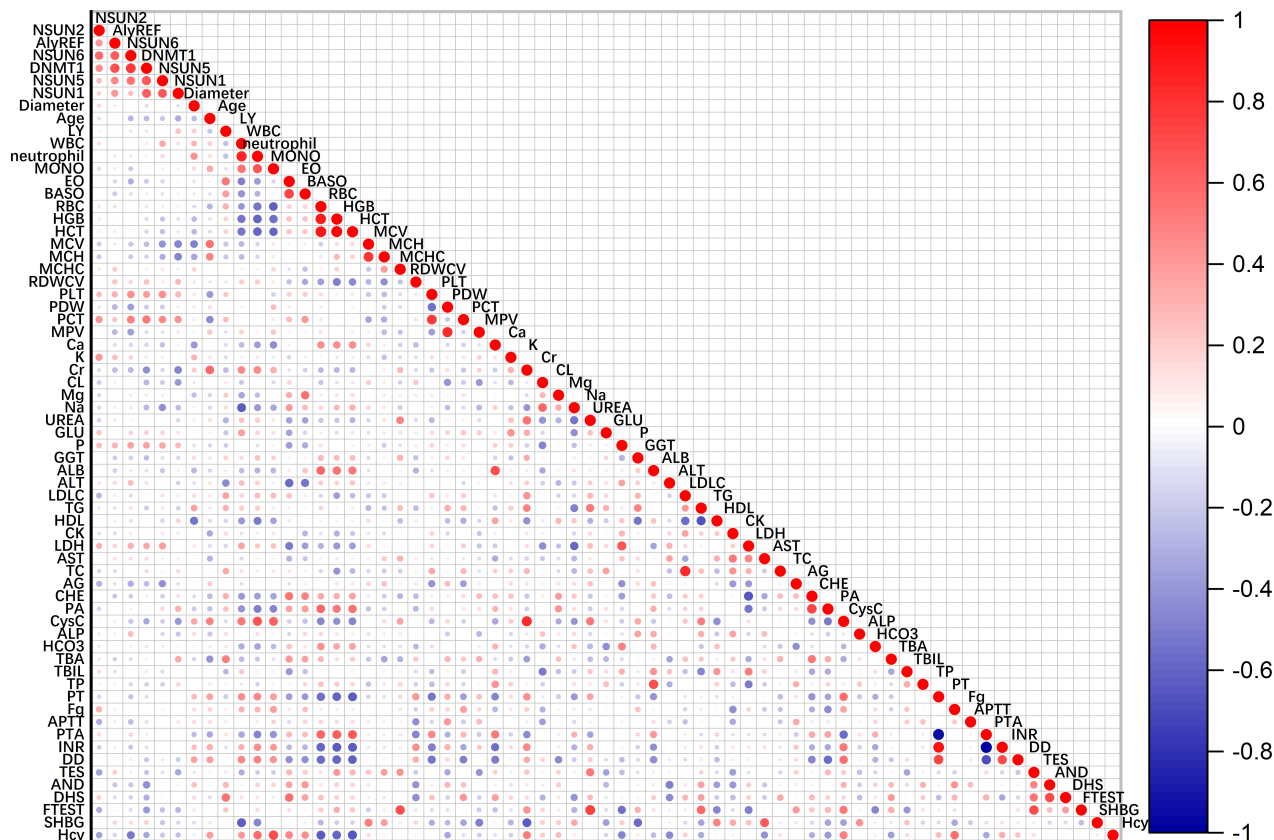
Fig. 2. Correlation among the mRNA expressions of m5C modulators and clinical parameters. Partial correlation analysis was adjusted with age, gender, BMI, and smoking. BMI, body mass index; LY, lymphocyte; WBC, white blood cell; MONO, monocyte; EO, eosinophils; BASO, basophil; RBC, red blood cell; HGB, hemoglobin; HCT, hematocrit; MCV, mean corpuscular volume; MCH, mean corpuscular hemoglobin; RDWCV, red blood cell volume distribution width; MCHC, mean corpuscular hemoglobin concentration; PLT, platelets; PDW, platelet distribution width; PCT, platelet hematocrit; MPV, mean platelet volume; Ca, serum calcium; K, serum kalium; Cr, creatinine; Cl, serum chlorine; Mg, serum magnesium; Na, serum sodium; GLU, fasting plasma glucose; P, serum phosphate; GGT, gamma glutamyl transpeptidase; ALB, albumin; ALT, alanine aminotransferase; LDL-C, low-density lipoprotein-cholesterol; TG, triglycerides; HDL-C, high-density lipoprotein-cholesterol; CK, creatine kinase; LDH, lactate dehydrogenase; AST, aspartate aminotransferase; TC, total cholesterol; AG, anion gap; CHE, cholinesterase; PA, pre-albumin; CysC, cystatin C; ALP, alkaline phosphatase; TBA, total bile acid; TBIL, total bilirubin; TP, total protein; PT, prothrombin time; Fg, fibrinogen; APTT, activated partial thromboplastin time; PTA, prothrombin activity; INR, international normalized ratio; DD, D-dimer; TES, testosterone; AND, androgen; DHS, dehydroepiandrosterone; F-TEST, free testosterone; SHBG, sex hormone-binding globulin; Hcy, Homocysteine.

staining showed weak colocalization with CD34+ ECs, and strongly with CD45+ leukocytes and CD3+ T lymphocytes. Aly/REF also showed strong colocalization with CD3+ T lymphocytes and CD45+ leukocytes (Fig. 3D).

Later, the AAA wall and normal aortic wall co-localization of Aly/REF with NSUN2 was examined using IF analysis (Fig. 3E). Here, we also observed that the expressions of NSUN2 and Aly/REF were higher in AAA sections compared with the controls. The result is similar to the results of western blot analysis and IHC analysis. Furthermore, for the co-localization analysis, NSUN2 and Aly/REF were co-expressed in the one cell in AAA group (Fig. 3E).

4.6 RIP-seq Identifies Aly/REF-interacting lncRNAs in AAA

The possible Aly/REF target genes were predicted by RIP-seq assay. lncRNAs have the length of over 200 nucleotides (nt). In addition, this study analyzed those known lncRNAs for their length distribution. As a result, there were markedly more lncRNAs with the length of 500–1000 and >3500 bp compared with those with additional lengths. Here, using RIP-seq, we detected a total of 36,224 lncRNAs in human AAA tissue. Afterwards, reads ≥1.0 or those with an anti-Aly/REF group to IgG control enrichment ratio >1.5 were screened; finally, 477 lncRNAs that bound to Aly/REF were discovered within AAA samples. For those upregulated lncRNAs, distributions among the human chromosomes were also illustrated in Fig. 4A. A total of 221 intergenic, 20 intron sense overlapping, 136 exon sense over-
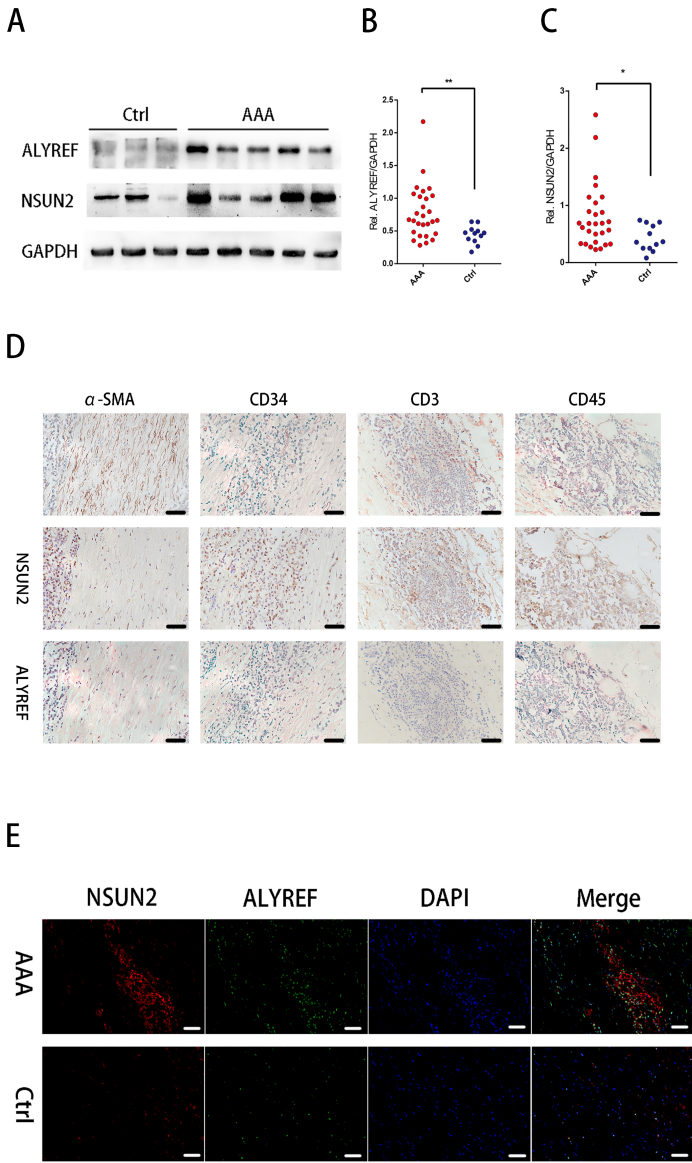
Fig. 3. Protein level of Aly/REF and NUSN2 are highly expressed in human abdominal aortic aneurysm (AAA). The representative images of blots between AAA and healthy aortas at the protein level (A); The density of the protein signals for Aly/REF (B) and NUSN2 (C) through the non-parametric Mann-Whitney U test quantification of the band intensities relative to the expression of GAPDH. *, $p < 0.05$; **, $p < 0.005$. The representative photographs of immunohistochemical staining for NSUN2, Aly/REF (D) and individual cell types markers in AAA tissue. Scale bar, 50 μm. AAA, abdominal aortic aneurysm; α-SMC, smooth muscle cell; CD34, endothelial cell and neovascularization; CD45, leukocytes; CD3, T lymphocytes. (E) Confocal immunofluorescence for human AAA sections stained with NUSN2, Aly/REF and 4', 6-diamidino-2-phenylindole (DAPI). AAA, specimens of abdominal aortic aneurysm ($N = 32$). Ctrl, control healthy aorta ($N = 12$).

lapping, 38 natural antisense, 43 intronic antisense, 19 bidirectional lncRNAs were identified (Fig. 4B), the lncRNA length of Aly/REF binding lncRNAs (Fig. 4C); and relationship of Aly/REF binding lncRNAs (Fig. 4D).

GO analysis indicated that the functions of Aly/REF-interacting lncRNA were involved in a variety of biological processes, including immune system process and macrophages infiltration, i.e., macrophage cytokine production (GO:0010934), immune system process (GO:0002376) for Biological Process; MHC class I protein complex (GO:0042612), platelet alpha granule (GO:0031091) for Cellular Component; and MHC class I protein binding (GO:0042288), MHC protein binding (GO:0042287) for Molecular Function (Fig. 5).

KEGG pathway analysis indicated the upregulation of 26 pathways, mainly including ECM-receptor interaction (KEGG: hsa04512), PPAR (KEGG: hsa03320) and phagosome (KEGG: hsa04145) signal transduction pathways, suggested that dysregulated lncRNA pathways in Aly/REF were closely associated with signal transduc-
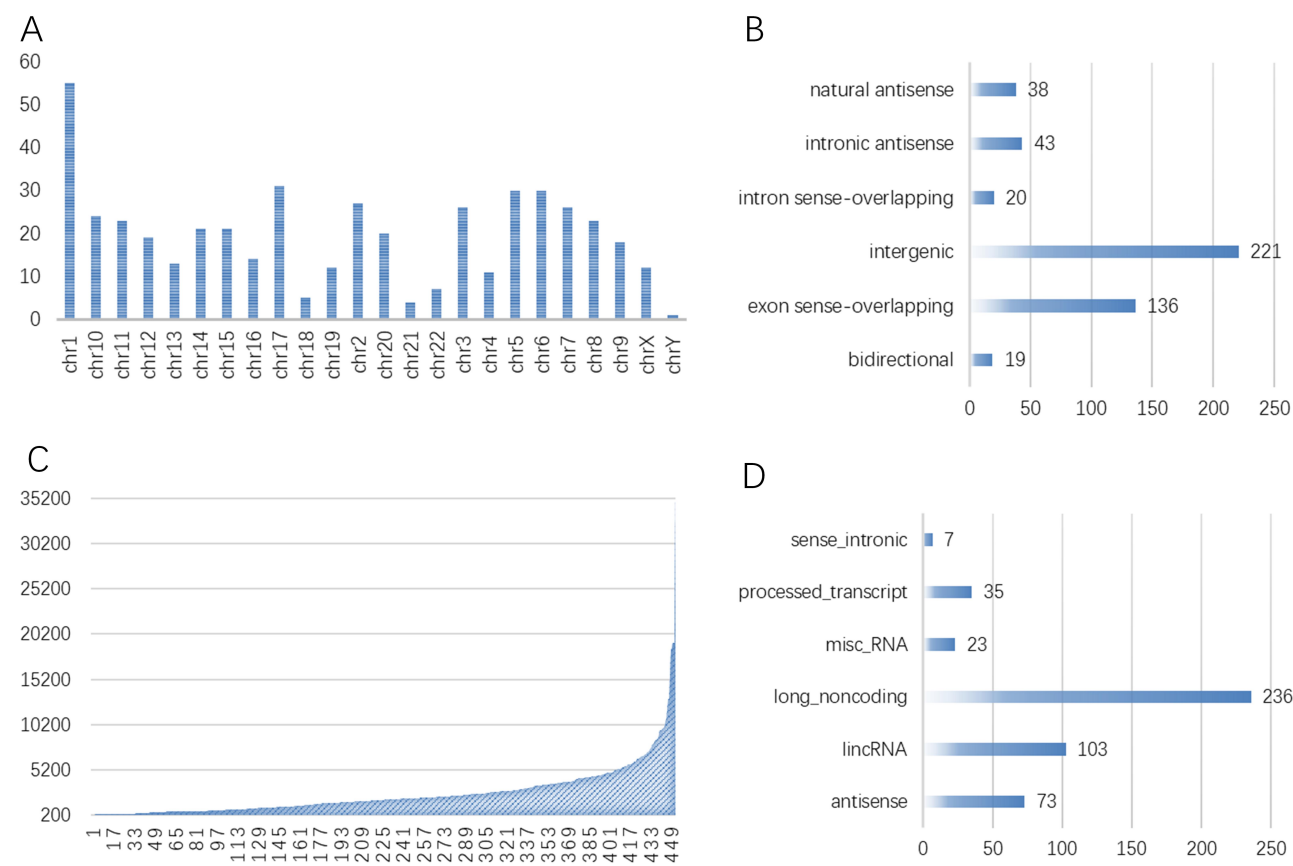
Fig. 4. The results demonstrated that 477 differentially expressed genes Aly/REF-binding lncRNAs in AAA tissue. The locus, genomic locus, chromosome of Aly/REF binding lncRNAs (A); the biotype of Aly/REF binding lncRNAs (B); the lncRNA length of Aly/REF binding lncRNAs (C); and relationship of Aly/REF binding lncRNAs (D) in abdominal aortic aneurysm tissue. Note, exon sense-overlapping: the LncRNA's exon is overlapping a coding transcript exon on the same genomic strand; intron sense-overlapping: the LncRNA is overlapping the intron of a coding transcript on the same genomic strand; intronic antisense: the LncRNA is overlapping the intron of a coding transcript on the antisense strand; natural antisense: the LncRNA is transcribed from the antisense strand and overlapping with a coding transcript; bidirectional: the LncRNA is oriented head-to-head to a coding transcript within 1000 bp; intergenic: there are no overlapping or bidirectional coding transcripts nearby the LncRNA.

tion in AAA tissue (**Supplementary Fig. 2**). Based on the FC, the top 20 dysregulated lncRNAs are summarized in Table 5. Among these dysregulated lncRNAs, distributions among the human chromosomes were also illustrated.

4.7 RIP-seq Identifies Aly/REF-interacting mRNAs in AAA

After RPKM value distribution was analyzed, we analyzed the sample gene expression profiles on the whole. When IP showed significant enrichment relative to input group, the combined expression for each gene of IP group increased relative to input group. Through RIP-seq, mapping data revealed that FMRP had 3060 potential target genes, which showed extensive activities in cell physiological processes, moreover, there were 369 mRNAs showing differential expression ($p < 0.01$) in AAA tissue (anti-Aly/REF group relative to IgG control).

To reduce the mRNAs binding to Aly/REF to better investigate and enrich mRNAs that might be related to AAA, this study screened the significantly differentially ex-pressed mRNAs (FC >4, $p < 0.01$) possibly related to the protein encoding genes annotated based on GO functional annotation and scientific literature. Based on the FC, the top 40 dysregulated mRNAs are summarized in Table 6. As expected, Dnmt1 was candidate mRNAs of Aly/REF-interacting mRNA by RIP-seq identified in AAA tissue.

GO analysis indicated that the functions of Aly/REF-interacting mRNA were related to various biological processes, such as UDP-N-acetylglucosamine metabolic process and endocytic recycling; and cellular component, including eukaryotic 48S preinitiation complex, eukaryotic 43S preinitiation complex; and platelet-derived growth factor biding, histone methyltansferases activity (**Supplementary Fig. 3**).

KEGG Moreover, regulated pathways were enriched in protein processing in endoplasmic reticulum (KEGG: hsa04141), lysine degradation (KEGG: hsa00310), and Focal adhesion (KEGG: hsa04510) (**Supplementary Fig. 4**).
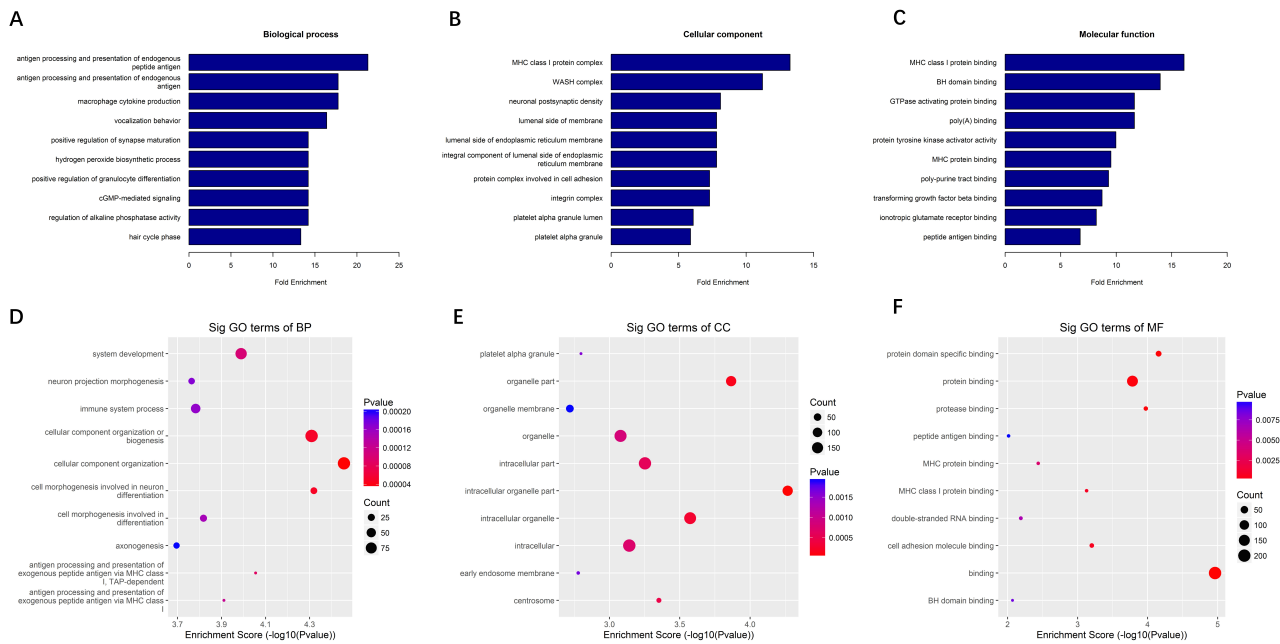
Fig. 5. Go analysis of 477 differentially expressed genes Aly/REF-binding lncRNAs in AAA tissue. Fold enrichment in biological process (A), cellular component (B), and molecular function (C); The enrichment score in biological process (D), cellular component (E), and molecular function (F).

Altogether 369 DEGs were analyzed against the STRING database. At the same time, Cytoscape was used to construct a PPI network through neighborhood, co-expression, settings experiments, text-mining and database. Afterwards, the separated genes were removed (those that did not interact with the remaining genes), and the DEGs regulated by Aly/REF were exhibited with 745 edges and 372 nodes (Fig. 6). Based on every gene degree, 4 hub genes that had a >20 degree were obtained, including ALB, ATM, TRIP12, and HIF1A.

4.8 Regulatory network (lncRNA-mRNA) analysis

Firstly, the lncRNA-mRNA correlations were analyzed based on 369 differentially expressed mRNAs and 477 differentially expressed lncRNAs. For better investigating the associations among the coding genes, the NI-ANA approach [28] was used for regulatory network analysis, which exhibited the network objects for the 246 candidate lncRNAs.

Secondly, we screened the candidates in the lncRNA-mRNA interaction network by the correlation >0.7 threshold, which yielded a network that consisted of 246 lncRNAs and 369 mRNAs (Fig. 7).

Similarly, 8 hub mRNA candidates (*SLC3A2, CCNL1, WDR81, MLLT10, BCL2L1, FHL1, GON4L, MYO15B*) also exerted vital parts in the regulatory network, as observed from Table 7. In addition, there were more genes and signaling pathways involved in the above constructed network, suggesting the complicated mechanisms by which Aly/REF-binding mRNAs and lncRNAs regulated the AAA pathogenic mechanism.

5. Discussion

AAA is one of the most severe vascular diseases in the vascular surgery [29, 30]. Because of the complex pathogenesis of AAA, efficient medical treatment for preventing the occurrence and rupture of AAA is lacking so far [31]. Among the researches on the AAA pathogenesis, epigenetic regulation occupies an increasing decisive position [32]. 5-methylcytosine modification on mRNA is a novel mRNA epigenetic modification, which have been found to play an essential role in other diseases [33, 34]. However, the evidence on the relationship between AAA and mRNA m5C modification is still lack. Therefore, this work aimed to examine the relationship of mRNA m5C expression with AAA. And for the first time, we observed that increased mRNA m5C modification occurred in AAA tissues, compared with the healthy controls.

Here, we observed up-regulating in the AAA tissue samples relative to matched normal tissues (>1.5-fold) at mRNA and protein level. Clinically, the NSUN2 expression was positively correlated to platelet hematocrit in AAA patients. NSUN2, firstly recognized as a tRNA m5C-methyltransferases [35], was also identified to methylate mRNA. Several researches have reported previously that NSUN2 regulated the stability, the translation of mRNAs and further affected gene expressions in cell proliferation [36], oxidative stress [37], inflammation reactions [38] and other pathophysiological processes [39]. These processes might participate in the progression of AAA [40] and other cardiovascular diseases [41]. Recently, Miao *et al.* [40] suggested that Nsun2 regulated hyperhomocysteinemia (HHcy)-deteriorated AAA progression mostly through

Table 4. The correlations among m5C status and m5C modulators.

	m5c	NSUN1	NSUN2	NSUN5	NSUN6	Dnmt1	Aly/REF
m5c	-						
	-						
NSUN1	−0.264	-					
	0.087	-					
NSUN2	0.316*	0.209	-				
	0.039	0.18	-				
NSUN5	0.320*	0.218	0.538**	-			
	0.037	0.16	<0.001	-			
NSUN6	−0.145	0.451**	0.287	0.410**	-		
	0.352	0.002	0.062	0.006	-		
Dnmt1	−0.099	0.470**	0.143	0.349*	0.673**	-	
	0.527	0.001	0.361	0.022	<0.001	-	
Aly/REF	0.312*	0.313*	0.464**	0.642**	0.214	0.339*	-
	0.042	0.041	0.002	<0.001	0.169	0.026	-

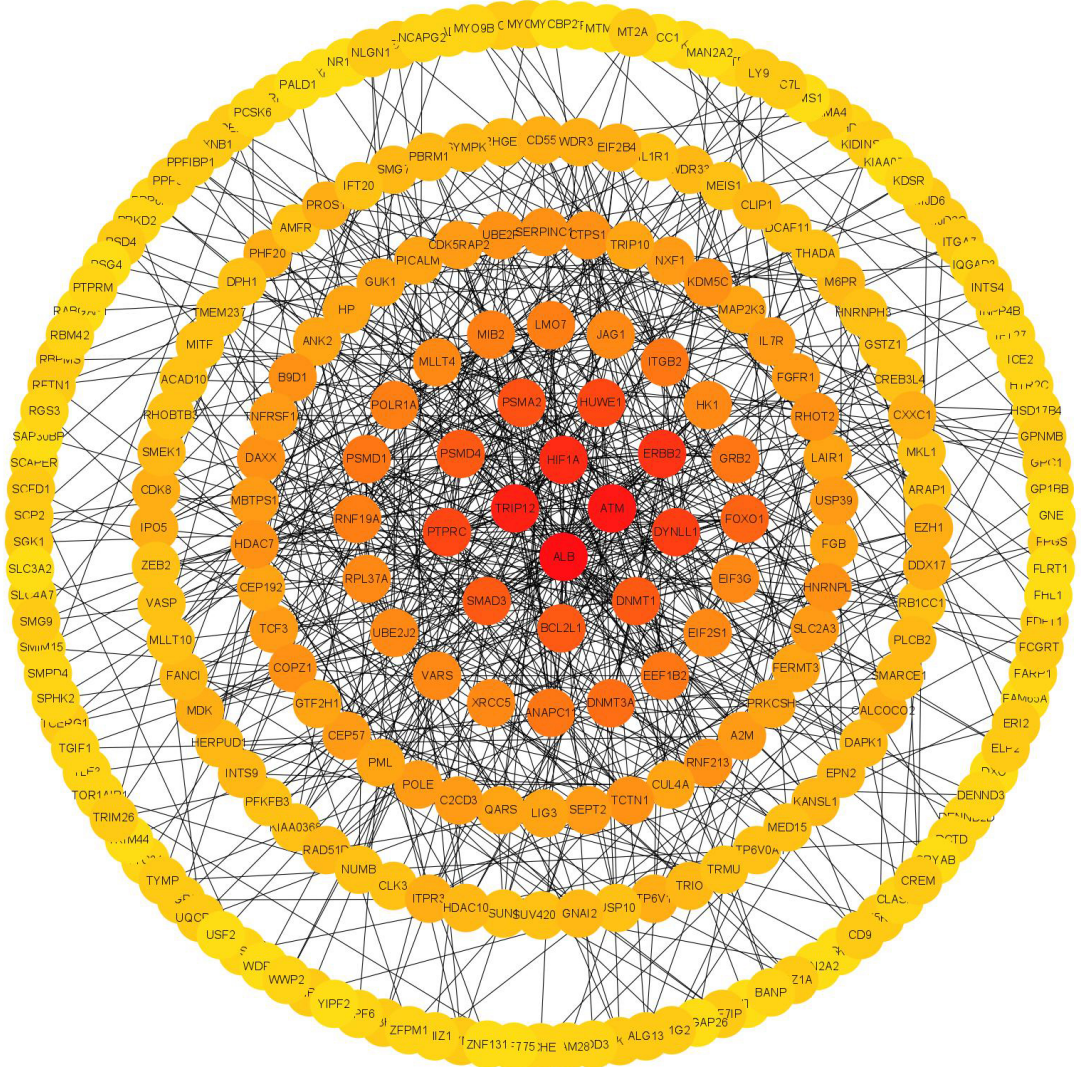Note, significant correlation: $*p < 0.05$, $**p < 0.01$, $***p < 0.001$.

Fig. 6. Construction of PPI network, analysis of 369 differentially expressed, and identification of hub genes.
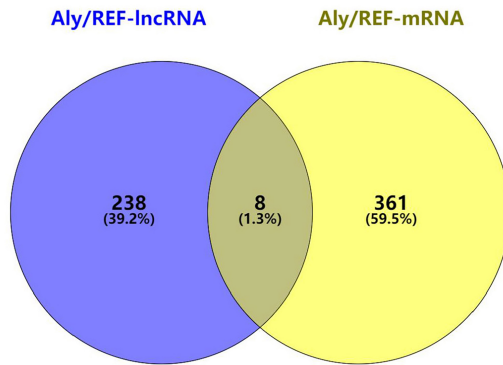
Fig. 7. The Venn diagram of the candidates in the lncRNA-mRNA interaction network. lncRNA and mRNAs were selected with a threshold of correlation >0.7, resulting in a network consisting 246 lncRNAs and 369 mRNAs.

elevating the expression and production of endothelial autotaxin, along with the migration of T cells, and this accounts for a new mechanism for the HHcy-deteriorated pathogenic mechanism and vascular inflammation in AAA. In the current study, we found that NSUN2 was higher within human AAA tissues relative to normal tissues, significantly correlated with m5C status of mRNA, and was localized in the inflammatory cells through IHC analysis. Our results indicated that NSUN2 may play an important role in the m5C methylation of mRNA in the AAA progression. Further research should focus on its potential function on regulating expressions of target genes in AAA, which may provide a new insight on the etiological study of abdominal aortic aneurysm.

Aly/REF is a specific mRNA m5C reader, which can bind to m5C sites in mRNA [33, 42], and contributes to the regulation of mRNA export [43]. *Aly/REF* plays a critical role on promoting the nuclear-cytoplasmic shuttling mRNA export in conjunction with NSUN2 [33]. It has been reported previously that either knock-down of *NSUN2* or knock-down of *Aly/REF* affected the cytoplasmic to nuclear ratios of mRNAs [36]. In the current study, we found a higher level of Aly/REF in AAA group. Additionally, the expression of Aly/REF was strongly correlated with m5C status of mRNAs and the expression of NSUN2. Furthermore, according to the IHC analysis and IF analysis, NSUN2 and Aly/REF were co-expressed in the inflammatory cells in AAA tissues, which illustrated that NSUN2 and Aly/REF might mediate mRNA m5C modification in inflammatory cells. Yang *et al.* [33] have suggested a similar point about m5C formation in mRNAs is mainly catalyzed by the RNA methyltransferase NSUN2, and m5C is specifically recognized by the mRNA export adaptor Aly/REF as shown by *in vitro* and *in vivo* studies. NSUN2 modulates Aly/REF's nuclear-cytoplasmic shuttling, RNA-binding affinity and associated mRNA export. The modification may be related with inflammatory infiltration in

AAA. It has been reported that NSUN2 regulated AAA formation by promoting T cell recruitment. However, the research on the association of inflammation with m5C modification and Aly/REF is still lack. Phenotypic transformation of immune cells is an important mechanism of AAA progression. Further researches should focus on the potential role of m5C modification in the phenotypic transformation of immune cells.

Considering the higher level of Aly/REF in AAA and its specific binding to mRNA m5C sites as identified by other researches, Aly/REF may play a critical role in the mRNA m5C status in AAA. Therefore, we tried to perform RIP-Sequence of Aly/REF in AAA tissues to find out the downstream target lncRNA and mRNA of Aly/REF. According to our result, in AAA tissue samples, the downstream mRNAs were involved in several pathophysiological processes. As this study explored, Dnmt1 was candidate mRNAs of Aly/REF-interacting mRNA by RIP-seq identified in AAA tissue. Previous study demonstrated that high Aly/REF expression and low DNMT1 expression were both associated with poor head and neck squamous cell carcinoma prognosis [44]. Simultaneously, the target differential expression mRNA regulated by Aly/REF were exhibited by PPI network, four hub genes were obtained, including *ALB, ATM, TRIP12,* and *HIF1A*. As well as Aly/REF-HIF1A interaction, a bioprocesses of bladder cancer cells were demonstrated by a series of experiments in vitro, they found that hypoxia-inducible factor-1alpha (HIF-1A) indirectly up-regulated the expression of PKM2 by activating Aly/REF in addition to activating its transcription directly [45]. Future cellular and molecular studies are required to further validate our findings and to better understand the genes targeted for m5C modifications during AAA progression.

For example, Aly/REF-interacting lncRNAs were associated with various biological processes, including immune system process and macrophages infiltration, i.e., macrophage cytokine production, MHC class I protein complex, MHC class I protein binding, and MHC protein binding. Meanwhile, lncRNAs also participated in Phagosome pathway, PPAR signaling pathway and ECM-receptor interaction pathway, which have been identified to be modulated in the current study. Long non-coding RNAs (lncRNAs), which are the main non-coding RNAs, are transcripts longer than 200 nt. They are known to play a key role in chromatin remodeling, transcription, and post-transcriptional regulation [46]. At present, few studies exist on m5C related lncRNAs. Studies have performed quantitative mapping of the m5C sites in Arabidopsis thaliana on a transcriptome range, and found more than 1000 m5C sites in mRNA, long non-coding RNA [47]. NSUN2 may play a similar role in lncRNAs. Sun *et al.* [48] showed that NSUN2 deficiency significantly decreased the half-life of H19 RNA (lncRNA), which might be regulated by NSUN2-mediated m5C modification in hepatocellular carcinoma.

Table 5. General information of top 20 ranked regulated long non-coding RNAs by Aly/REF-binding.

No.	Transcript ID	Biotype	Strand	Gene ID	Chromosome	LncRNA Source	LncRNA length	Relationship	Association gene name
1	ENST00000416191	antisense	+	ENSG00000258486	chr14	Ensembl	297	bidirectional	*RPS29*
2	ENST00000598952	misc RNA	−	ENSG00000265150	chr14	Ensembl	297	intergenic	
3	uc003ine.3	lincRNA	−	ENSG00000260402	chr16	Ensembl	2484	intergenic	
4	ENST00000473958	misc RNA	−	ENSG00000200488	chr2	Ensembl	332	intergenic	
5	TCONS_l2_00025918	misc RNA	+	ENSG00000265735	chr9	Ensembl	288	intronic antisense	*PTPRD*
6	uc009ykc.1	lincRNA	+	ENSG00000224934	chr10	Ensembl	2998	bidirectional	*GOT1*
7	ENST00000455068	antisense	+	ENSG00000269296	chr19	Ensembl	3653	natural antisense	*ZNF780A*
8	ENST00000493013	long noncoding	−	BC039551	chr4	UCSC knowngene	1124	intronic antisense	*FHDC1*
9	TCONS_00004186	antisense	+	ENSG00000244300	chr3	Ensembl	722	intronic antisense	*GATA2*
10	ENST00000565978	long noncoding	−	SNHG10	chr14	RefSeq	1980	bidirectional	*GLRX5*
11	ENST00000510986	antisense	−	ENSG00000225733	chr3	Ensembl	1874	intronic antisense	*NR2C2*
12	uc002xuq.1	lincRNA	−	ENSG00000267427	chr19	Ensembl	2103	exon sense-overlapping	*MLLT1*
13	ENST00000516507	antisense	−	ENSG00000249042	chr5	Ensembl	1151	bidirectional	*FAM151B*
14	ENST00000586625	antisense	+	ENSG00000259985	chr18	Ensembl	1169	natural antisense	*B4GALT6*
15	TCONS_l2_00005763	lincRNA	+	ENSG00000254339	chr8	Ensembl	697	intergenic	
16	NR104639	long noncoding	−	CENPJ	chr13	RefSeq	5246	exon sense-overlapping	*CENPJ*
17	ENST00000332012	lincRNA	+	ENSG00000248587	chr5	Ensembl	1941	exon sense-overlapping	*GDNF-AS1*
18	ENST00000556819	long noncoding	−	AK055386	chr20	UCSC knowngene	3404	intergenic	
19	ENST00000602575	antisense	+	ENSG00000227061	chr2	Ensembl	4775	intergenic	
20	ENST00000434707	processed transcript	+	ENSG00000012171	chr13	Ensembl	1765	exon sense-overlapping	*SEMA3B*

Table 6. General information of top 40 ranked regulated mRNAs by Aly/REF-binding.

No.	Gene symbol	Gene ID	Strand	Chromosome	Map location	Gene name
1	*MYCBP2*	ENSG00000005810	−	13	13q22	MYC binding protein 2, E3 ubiquitin protein ligase
2	*LUC7L*	ENSG00000007392	−	16	16p13.3	LUC7-like
3	*TYMP*	ENSG00000025708	−	22	22q13.33	thymidine phosphorylase
4	*CYFIP2*	ENSG00000055163	+	5	5q33.3	cytoplasmic FMR1 interacting protein 2
5	*MYO9A*	ENSG00000066933	−	15	15q22-q23	myosin IXA
6	*JMJD6*	ENSG00000070495	−	17	17q25	jumonji domain containing 6
7	*FGFR1*	ENSG00000077782	−	8	8p11.23-p11.22	fibroblast growth factor receptor 1
8	*SDF4*	ENSG00000078808	−	1	1p36.33	stromal cell derived factor 4
9	*CREM*	ENSG00000095794	+	10	10p11.21	cAMP responsive element modulator
10	*MED15*	ENSG00000099917	+	22	22q11.2	mediator complex subunit 15
11	*ZC3H14*	ENSG00000100722	+	14	14q31.3	zinc finger CCCH-type containing 14
12	*DCAF11*	ENSG00000100897	+	14	14q11.2	DDB1 and CUL4 associated factor 11
13	*ZMYND8*	ENSG00000101040	−	20	20q13.12	zinc finger MYND-type containing 8
14	*SIRPB1*	ENSG00000101307	−	20	20p13	signal regulatory protein beta 1
15	*JAG1*	ENSG00000101384	−	20	20p12.1-p11.23	jagged 1
16	*MTMR9*	ENSG00000104643	+	8	8p23-p22	myotubularin related protein 9
17	*VRK3*	ENSG00000105053	−	19	19q13	vaccinia related kinase 3
18	*PALD1*	ENSG00000107719	+	10	10q22.1	phosphatase domain containing, paladin 1
19	*XPNPEP1*	ENSG00000108039	−	10	10q25.3	X-prolyl aminopeptidase (aminopeptidase P) 1, soluble
20	*ZMIZ1*	ENSG00000108175	+	10	10q22.3	zinc finger MIZ-type containing 1
21	*CDK5RAP3*	ENSG00000108465	+	17	17q21.32	CDK5 regulatory subunit associated protein 3
22	*PPP6R3*	ENSG00000110075	+	11	11q13	protein phosphatase 6 regulatory subunit 3
23	*ELMOD3*	ENSG00000115459	+	2	2p11.2	ELMO/CED-12 domain containing 3
24	*SERPINC1*	ENSG00000117601	−	1	1q25.1	serpin peptidase inhibitor, clade C (antithrombin), member 1
25	*MTRR*	ENSG00000124275	+	5	5p15.31	5-methyltetrahydrofolate-homocysteine methyltransferase reductase
26	*ERMARD*	ENSG00000130023	+	6	6q27	ER membrane-associated RNA degradation
27	*YIPF2*	ENSG00000130733	−	19	19p13.2	Yip1 domain family member 2
28	*DNMT1*	ENSG00000130816	−	19	19p13.2	DNA (cytosine-5-)-methyltransferase 1
29	*SCLY*	ENSG00000132330	+	2	2q37.3	selenocysteine lyase
30	*HSD17B4*	ENSG00000133835	+	5	5q21	hydroxysteroid (17-beta) dehydrogenase 4
31	*NUMB*	ENSG00000133961	−	14	14q24.3	numb homolog (Drosophila)
32	*ZCCHC11*	ENSG00000134744	−	1	1p32.3	zinc finger CCHC-type containing 11
33	*ELP2*	ENSG00000134759	+	18	18q12.2	elongator acetyltransferase complex subunit 2
34	*LMO7*	ENSG00000136153	+	13	13q22.2	LIM domain 7
35	*CALCOCO2*	ENSG00000136436	+	17	17q21.32	calcium binding and coiled-coil domain 2
36	*FPGS*	ENSG00000136877	+	9	9q34.1	folylpolyglutamate synthase
37	*PML*	ENSG00000140464	+	15	15q22	promyelocytic leukemia
38	*RHOT2*	ENSG00000140983	+	16	16p13.3	ras homolog family member T2
39	*DEF8*	ENSG00000140995	+	16	16q24.3	differentially expressed in FDCP 8 homolog (mouse)
40	*ANAPC11*	ENSG00000141552	+	17	17q25.3	anaphase promoting complex subunit 11

Table 7. The 8 hub mRNA candidates in the lncRNA-mRNA interaction network.

Transcript ID	Biotype	Strand	Gene ID	Locus	LncRNA Source	LncRNA length	Associated gene transID	Association gene name
ENST00000363981	processed transcript	−	ENSG00000255717	chr11:62619459-62623386	Ensembl	72	ENST00000377892	*SLC3A2*
ENST00000364908	misc RNA	+	ENSG00000201778	chr3:156864296-156878549	Ensembl	93	NM001308185	*CCNL1*
ENST00000571091	lincRNA	−	ENSG00000186594	chr17:1614804-1641893	Ensembl	525	ENST00000446363	*WDR81*
uc001irb.3	long noncoding	+	MLLT10	chr10:21823093-22032559	UCSC knowngene	3611	ENST00000307729	*MLLT10*
uc002wwk.3	long noncoding	−	BCL2L1	chr20:30252254-30311792	UCSC knowngene	2462	ENST00000376062	*BCL2L1*
uc004ezm.2	long noncoding	+	FHL1	chrX:135228860-135293518	UCSC knowngene	2136	ENST00000345434	*FHL1*
uc009wrg.1	long noncoding	−	GON4L	chr1:155579566-155829191	UCSC knowngene	4500	ENST00000271883	*GON4L*
uc010dgi.1	long noncoding	+	MYO15B	chr17:73584138-73704142	UCSC knowngene	3088	ENST00000578462	*MYO15B*

mRNA

Association gene name	Description	Deneid	Strand	Locus	RIP FPKM	Gene ID	Chromosome	Map location
SLC3A2	solute carrier family 3 member 2	ENSG00000168003	+	chr11:62623517-62656355	14.1648	6520	11	11q13
CCNL1	cyclin L1	ENSG00000163660	−	chr3:156864296-156878549	27.0217	57018	3	3q25.31
WDR81	WD repeat domain 81	ENSG00000167716	+	chr17:1614804-1641893	46.204	124997	17	17p13.3
MLLT10	myeloid/lymphoid or mixed-lineage leukemia; translocated to, 10	ENSG00000078403	+	chr10:21823093-22032559	14.4303	8028	10	10p12
BCL2L1	BCL2 like 1	ENSG00000171552	−	chr20:30252254-30311792	26.9695	598	20	20q11.21
FHL1	four and a half LIM domains 1	ENSG00000022267	+	chrX:135228860-135293518	166.2	2273	X	Xq26
GON4L	gon-4-like (C. elegans)	ENSG00000116580	−	chr1:155579566-155829191	42.58	54856	1	1q22
MYO15B	myosin XVB	ENSG00000266714	+	chr17:73584138-73704142	230.939	80022	17	17q25.1

Note, RIP vs IgG.

FPKM, fragments per kilobase of transcript per million mapped reads.

Nevertheless, the mechanism of m5C methylation in lncR-NAs promoting AAA progress is unclear, and deeper exploration would be helpful for understanding the pathogenesis of AAA.

Through bioinformation method, we also predicted eight hub mRNA candidates (SLC3A2, CCNL1, WDR81, MLLT10, BCL2L1, FHL1, GON4L, MYO15B) exerted vital parts in the lncRNAs-mRNAs regulation network. The sequence profile provided reliable basis for the mechanism of m5C methylation regulating AAA progression. However, further researches are needed to focus on the relationship of m5C target RNA and AAA, which may uncover a new cause of AAA occurrence.

6. Conclusions

We were first to observe m5A modification in human abdominal aortic aneurysm tissues. The results also reveal the important roles of m5C modulators, including NUSN2 and Aly/REF, in the pathogenesis of human AAA and provide a new view on m5C modification in AAA. Our findings suggest a potential mechanism of RNA methylation modification in clinical AAA. Understanding how these m5C RNA modifications occur, and the correlation between lncRNA changes in structure and function, may open up new therapeutic possibilities in AAA. Future molecular and cellular studies are required to further identify our findings and to better understand the genes targeted for m5C RNA methylation modifications during AAA progression.

7. Author contributions

Conceptualization—JZ and YSH; methodology—YCH, FXY and YHW; software—YSH and YCH; formal analysis—SYW, YSH and YCH; investigation—JZ and YSH; data curation— HZ and YCH; writing-original draft preparation—PPG, YCH and YSH; writing-review and editing—SJX and JZ; supervision—JZ and YSH; funding acquisition—YSH and JZ. All authors have read and agreed to the published version of the manuscript.

8. Ethics approval and consent to participate

Human AAA samples collection conducted according to the Guidelines of the World Medical Association Declaration of Helsinki, and was approved by the Ethics Committees of First Hospital of China Medical University (ethical approval number: 2019-97-2).

9. Acknowledgment

We thank Cloud-Seq Biotech Ltd. Co. (Shanghai, China) for the RIP-transcriptome sequencing service and the subsequent bioinformatics analysis.

10. Funding

11. Conflict of interest

The authors declare no conflict of interest.

12. Availability of data and materials

The datasets used and analyzed during the current study are available from the corresponding author on reasonable request. The datasets generated and/or analyzed during the current study are available in the Gene Expression Omnibus (GEO, http://www.ncbi.nlm.nih.gov/geo/) database (Accession Number: GSE 163615).

13. References

[1] Golledge J. Abdominal aortic aneurysm: update on pathogenesis and medical treatments. Nature Reviews Cardiology. 2019; 16: 225–242.

[2] Aronow WS. Peripheral arterial disease and abdominal aortic aneurysm in elderly people. Minerva Medica. 2011; 102: 483–500.

[3] Thompson RW, Geraghty PJ, Lee JK. Abdominal aortic aneurysms: basic mechanisms and clinical implications. Current Problems in Surgery. 2002; 39: 110–230.

[4] Eckstein H, Bruckner T, Heider P, Wolf O, Hanke M, Niedermeier H, et al. The relationship between volume and outcome following elective open repair of abdominal aortic aneurysms (AAA) in 131 German hospitals. European Journal of Vascular and Endovascular Surgery. 2007; 34: 260–266.

[5] Han Y, Zhang S, Zhang J, Ji C, Eckstein H. Outcomes of Endovascular Abdominal Aortic Aneurysm Repair in Octogenarians: Meta-analysis and Systematic Review. European Journal of Vascular and Endovascular Surgery. 2018; 54: 454–463.

[6] Trenner M, Haller B, Storck M, Reutersberg B, Kallmayer MA, Eckstein H. Trends in Patient Safety of Intact Abdominal Aortic Aneurysm Repair: German Registry Data on 36,594 Procedures. European Journal of Vascular and Endovascular Surgery. 2017; 53: 641–647.

[7] Moll FL, Powell JT, Fraedrich G, Verzini F, Haulon S, Waltham M, et al. Management of Abdominal Aortic Aneurysms Clinical Practice Guidelines of the European Society for Vascular Surgery. European Journal of Vascular and Endovascular Surgery. 2011; 41: S1–S58.

[8] Longo GM, Buda SJ, Fiotta N, Xiong W, Griener T, Shapiro S, et al. MMP-12 has a role in abdominal aortic aneurysms in mice. Surgery. 2005; 137: 457–462.

[9] Hellenthal FAMVI, Buurman WA, Wodzig WKWH, Schurink GWH. Biomarkers of abdominal aortic aneurysm progression.

Part 2: inflammation. Nature Reviews Cardiology. 2009; 6: 543–552.

[10] Lu WW, Jia LX, Ni XQ, Zhao L, Chang JR, Zhang JS, *et al*. Intermedin1-53 Attenuates Abdominal Aortic Aneurysm by Inhibiting Oxidative Stress. Arteriosclerosis, Thrombosis, and Vascular Biology. 2016; 36: 2176–2190.

[11] Hellenthal FAMVI, Buurman WA, Wodzig WKWH, Schurink GWH. Biomarkers of AAA progression. Part 1: extracellular matrix degeneration. Nature Reviews Cardiology. 2009; 6: 464–474.

[12] Bogunovic N, Meekel JP, Micha D, Blankensteijn JD, Hordijk PL, Yeung KK. Impaired smooth muscle cell contractility as a novel concept of abdominal aortic aneurysm pathophysiology. Scientific Reports. 2019; 9: 6837.

[13] Ryer EJ, Ronning KE, Erdman R, Schworer CM, Elmore JR, Peeler TC, *et al*. The potential role of DNA methylation in abdominal aortic aneurysms. International Journal of Molecular Sciences. 2015; 16: 11259–11275.

[14] Han Y, Tanios F, Reeps C, Zhang J, Schwamborn K, Eckstein H, *et al*. Histone acetylation and histone acetyltransferases show significant alterations in human abdominal aortic aneurysm. Clinical Epigenetics. 2016; 8: 3.

[15] Maegdefessel L, Spin JM, Raaz U, Eken SM, Toh R, Azuma J, *et al*. MiR-24 limits aortic vascular inflammation and murine abdominal aneurysm development. Nature Communications. 2016; 5: 5214.

[16] Covelo-Molares H, Bartosovic M, Vanacova S. RNA methylation in nuclear pre-mRNA processing. Wiley Interdisciplinary Reviews: RNA. 2018; 9: e1489.

[17] Dominissini D, Moshitch-Moshkovitz S, Schwartz S, Salmon-Divon M, Ungar L, Osenberg S, *et al*. Topology of the human and mouse m6a RNA methylomes revealed by m6a-seq. Nature. 2012; 485: 201–206.

[18] He Y, Xing J, Wang S, Xin S, Han Y, Zhang J. Increased m6a methylation level is associated with the progression of human abdominal aortic aneurysm. Annals of Translational Medicine. 2019; 7: 797–797.

[19] Trixl L, Lusser A. The dynamic RNA modification 5-methylcytosine and its emerging role as an epitranscriptomic mark. Wiley Interdisciplinary Reviews: RNA. 2019; 10: e1510.

[20] Haag S, Warda AS, Kretschmer J, Günnigmann MA, Höbartner C, Bohnsack MT. NSUN6 is a human RNA methyltransferase that catalyzes formation of m5C72 in specific tRNAs. RNA. 2015; 21: 1532–1543.

[21] Bohnsack KE, Hobartner C, Bohnsack MT. Eukaryotic 5-methylcytosine (m(5)C) RNA Methyltransferases: Mechanisms, Cellular Functions, and Links to Disease. Genes. 2019; 10: 102.

[22] Ilango S, Paital B, Jayachandran P, Padma PR, Nirmaladevi R. Epigenetic alterations in cancer. Frontiers in Bioscience. 2020; 25: 1058–109.

[23] Hu M, Hu M, Zhang Q, Lai J, Liu X. SETD2, an epigenetic tumor suppressor: a focused review on GI tumor. Frontiers in Bioscience. 2020; 25: 781–797.

[24] Tang DJ, Han YS, Lun Y, Jiang H, Xin SJ, Duan ZQ, *et al*. Y chromosome loss is associated with age-related male patients with abdominal aortic aneurysms. Clinical Interventions in Aging. 2019; 14: 1227–1241.

[25] Paraskevas KI, Eckstein H, Schermerhorn ML. Guideline Recommendations for the Management of Abdominal Aortic Aneurysms. Angiology. 2019; 70: 688–689.

[26] Zhao J, Sun BK, Erwin JA, Song J, Lee JT. Polycomb proteins targeted by a short repeat RNA to the mouse X chromosome. Science. 2008; 322: 750–756.

[27] Trapnell C, Williams BA, Pertea G, Mortazavi A, Kwan G, van Baren MJ, *et al*. Transcript assembly and quantification by RNA-Seq reveals unannotated transcripts and isoform switching during cell differentiation. Nature Biotechnology. 2010; 28: 511–515.

[28] Paraskevopoulou MD, Georgakilas G, Kostoulas N, Reczko M, Maragkakis M, Dalamagas TM, *et al*. DIANA-LncBase: experimentally verified and computationally predicted microRNA targets on long non-coding RNAs. Nucleic Acids Research. 2013; 41: D239–D245.

[29] Ullery BW, Hallett RL, Fleischmann D. Epidemiology and contemporary management of abdominal aortic aneurysms. Abdominal Radiology. 2018; 43: 1032–1043.

[30] Golledge J, Norman PE. Pathophysiology of abdominal aortic aneurysm relevant to improvements in patients' management. Current Opinion in Cardiology. 2009; 24: 532–538.

[31] Rahimtoola SH. Diagnosis and monitoring of abdominal aortic aneurysm: current status and future prospects. Foreword. Current Problems in Cardiology. 2011; 35: 509.

[32] Toghill BJ, Saratzis A, Freeman PJ, Sylvius N, Bown MJ. SMYD2 promoter DNA methylation is associated with abdominal aortic aneurysm (AAA) and SMYD2 expression in vascular smooth muscle cells. Clinical Epigenetics. 2018; 10: 29.

[33] Yang X, Yang Y, Sun B, Chen Y, Xu J, Lai W, *et al*. 5-methylcytosine promotes mRNA export - NSUN2 as the methyltransferase and ALYREF as an m5C reader. Cell Research. 2017; 27: 606–625.

[34] Squires JE, Patel HR, Nousch M, Sibbritt T, Humphreys DT, Parker BJ, *et al*. Widespread occurrence of 5-methylcytosine in human coding and non-coding RNA. Nucleic Acids Research. 2012; 40: 5023–5033.

[35] Shinoda S, Kitagawa S, Nakagawa S, Wei F, Tomizawa K, Araki K, *et al*. Mammalian NSUN2 introduces 5-methylcytidines into mitochondrial tRNAs. Nucleic Acids Research. 2019; 47: 8734–8745.

[36] Xu X, Zhang Y, Zhang J, Zhang X. NSun2 promotes cell migration through methylating autotaxin mRNA. Journal of Biological Chemistry. 2020; 295: 18134–18147.

[37] Gkatza NA, Castro C, Harvey RF, Heiss M, Popis MC, Blanco S, *et al*. Cytosine-5 RNA methylation links protein synthesis to cell metabolism. PLOS Biology. 2019; 17: e3000297.

[38] Luo Y, Feng J, Xu Q, Wang W, Wang X. NSun2 Deficiency Protects Endothelium from Inflammation via mRNA Methylation of ICAM-1. Circulation Research. 2016; 118: 944–956.

[39] Chellamuthu A, Gray SG. The RNA Methyltransferase NSUN2 and Its Potential Roles in Cancer. Cells. 2020; 9: 1758.

[40] Miao Y, Zhao Y, Han L, Ma X, Deng J, Yang J, *et al*. NSun2 regulates aneurysm formation by promoting autotaxin expression and T cell recruitment. Cellular and Molecular Life Sciences. 2020; 78: 1709–1727.

[41] Wang N, Tang H, Wang X, Wang W, Feng J. Homocysteine upregulates interleukin-17a expression via NSun2-mediated RNA methylation in T lymphocytes. Biochemical and Biophysical Research Communications. 2017; 493: 94–99.

[42] Fan J, Wang K, Du X, Wang J, Chen S, Wang Y, *et al*. ALYREF links 3'-end processing to nuclear export of non-polyadenylated mRNAs. EMBO J. 2019; 38: e99910.

[43] Shi M, Zhang H, Wu X, He Z, Wang L, Yin S, *et al*. ALYREF mainly binds to the 5' and the 3' regions of the mRNA *in vivo*. Nucleic Acids Research. 2017; 45: 9640–9653.

[44] Xue M, Shi Q, Zheng L, Li Q, Yang L, Zhang Y. Gene signatures of m5C regulators may predict prognoses of patients with head and neck squamous cell carcinoma. American Journal of Translational Research. 2020; 12: 6841–6852.

[45] Wang JZ, Zhu W, Han J, Yang X, Zhou R, Lu HC, *et al*. The role of the HIF-1alpha/ALYREF/PKM2 axis in glycolysis and tumorigenesis of bladder cancer. Cancer Communications. 2021; 41: 560–575.

[46] Li DY, Busch A, Jin H, Chernogubova E, Pelisek J, Karlsson J, *et al*. H19 Induces Abdominal Aortic Aneurysm Development and Progression. Circulation. 2018; 138: 1551–1568.

[47] David R, Burgess A, Parker B, Li J, Pulsford K, Sibbritt T, *et al*. Transcriptome-Wide Mapping of RNA 5-Methylcytosine in Arabidopsis mRNAs and Noncoding RNAs. The Plant Cell. 2017; 29: 445–460.

[48] Sun Z, Xue S, Zhang M, Xu H, Hu X, Chen S, *et al*. Aberrant NSUN2-mediated m5C modification of H19 lncRNA is associated with poor differentiation of hepatocellular carcinoma. Oncogene. 2020; 39: 6906–6919.

Send correspondence to:

Yanshuo Han, School of Life and Pharmaceutical Sciences, Dalian University of Technology, 116001 Dalian, Liaoning, China, E-mail: yanshuohan@dlut.edu.cn

Jian Zhang, Department of Vascular Surgery, The First Hospital of China Medical University, 110001 Shenyang, Liaoning, China, E-mail: jianzhang@cmu.edu.cn

[†] These authors contributed equally.